Studying the couplings of the Higgs boson to fermions with ATLAS

Higgs Hunting 2021

20th September 2021

Andy Chisholm (University of Birmingham)
on behalf of the ATLAS collaboration

This project has received funding from the European Union's Horizon 2020 research and innovation programme under grant agreement No. 714893 (ExclusiveHiggs)

The fermion masses appear randomly chosen and span orders of magnitude - why?

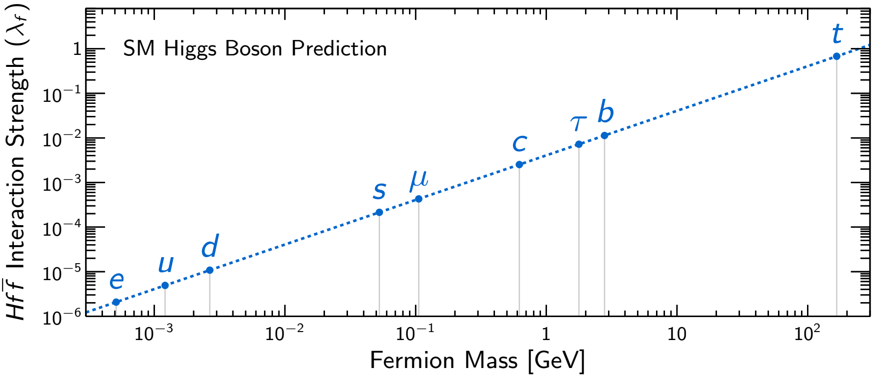

- The Yukawa sector of the SM offers no fundamental insight into the fermion mass hierarchy, there is something more to understand!
- Establishing and measuring the coupling of the Higgs boson with all of the fermions is a top priority for the LHC - do they all behave as the SM predicts?

The following talk will outline the current status of the ATLAS effort to study the couplings of the Higgs boson with the fermions, focussing on the latest results

$t\bar{t}H$ production (ATLAS-CONF-2020-058 and PRL 125 (2020) 061802)

Strongest Yukawa coupling probed directly with the $t\bar{t}H$ production, dedicated analyses with full Run 2 dataset available in $H \to b\bar{b}$ and $H \to \gamma\gamma$ channels...

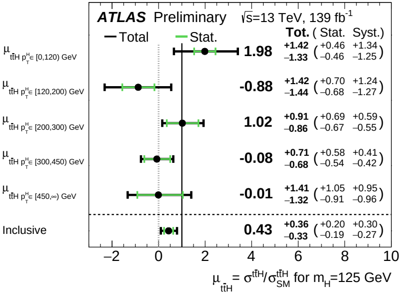

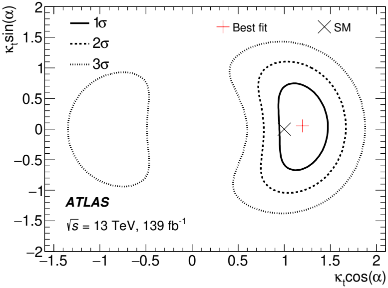

High $H \to b\bar{b}$ decay rate facilitates differential measurements of $t\bar{t}H$ production in STXS p_T^H bins

- Observed (expected) significance of $t\bar{t}H$ production 1.3 (3.0) σ

Also studied in multi-lepton final state and in context of $H \to 4\ell$ and $H \to \gamma\gamma$ coupling analyses (see EPJC 80 (2020) 957 and ATLAS-CONF-2020-026)

- $t\bar{t}H$ production confirmed at 5.2 σ (assuming CP-even coupling of SM)
- Pure CP-odd coupling $t\bar{t}H$ coupling excluded at 3.9 σ and CP-mixing angles $|\alpha| > 43^\circ$ excluded at 95% CL

Using $H \to \gamma\gamma$, CP nature of $t\bar{t}H$ coupling measured as very consistent with SM prediction

$VH, H \to b\bar{b}$ extensively studied using full Run 2 dataset in both resolved and merged (boosted) $H \to b\bar{b}$ decay topologies, with complementary p_T^H acceptance

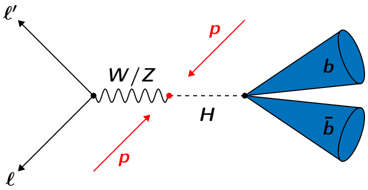

Resolved Strategy

EPJC 81 (2021) 178

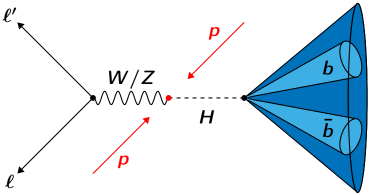

Boosted Strategy

PLB 816 (2021) 136204

- $H \to b\bar{b}$ system reconstructed with two $R = 0.4$ anti-k_T calorimeter jets
- Both jets required to be b-tagged
- Designed to be optimal for $p_T^V > 75$ GeV, bulk of cross-section at lower p_T^V

STXS p_T^V bins: $150 - 250, 250+$ GeV for both *ZH* and *WH* (also $75 - 150$ GeV for *ZH* only)

- $H \to b\bar{b}$ system reconstructed with single $R = 1.0$ anti-k_T calorimeter jet
- System identified with two b-tagged variable radius track jets, within the $R = 1.0$ jet
- Targets $p_T^V > 250$ GeV "boosted" topology where b-jets begin to merge

STXS p_T^V bins: $250 - 400, 400+$ GeV for both *ZH* and *WH*

The two separate analyses have now been carefully combined to measure two additional STXS bins and extend the sensitivity of the EFT interpretation!

- Significant overlap in the acceptance between the two analyses presents a challenge! $\to$
- Combination is performed by using resolved strategy for $p_T^V < 400$ GeV and boosted for $p_T^V > 400$ GeV
- Experimental uncertainties correlated between analyses (except b-tagging)
- Background modelling uncertainties generally treated as uncorrelated
- $V+$jets floating normalisation parameters coupled to better constrain uncertainties with data

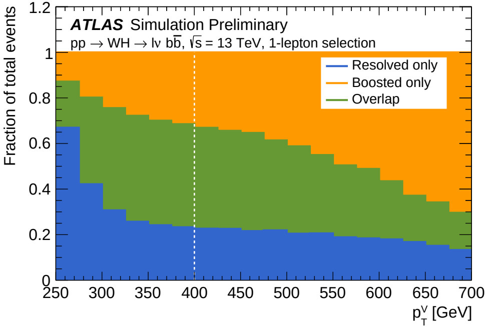

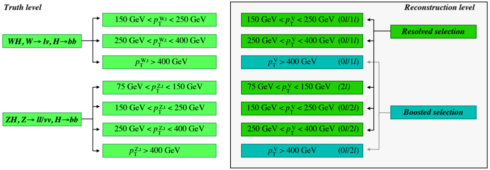

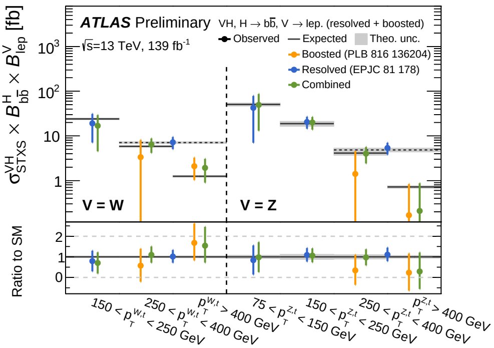

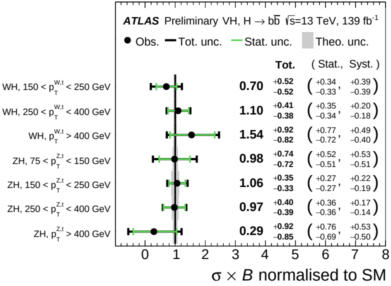

- Correlations between measured bins typically a few % and up to 10-15% for $p_T^V > 400$ GeV
- Statistical and systematic uncertainties comparable for $p_T^V < 400$ GeV, while statistical uncertainties limit sensitivity in highest p_T^V bins

STXS measurements of *WH* and *ZH* production from both analyses now harmonised to derive an extended comprehensive p_T^V measurement!

STXS p_T^V measurements interpreted in terms of an effective lagrangian (SMEFT) considering only $D = 6$ operators

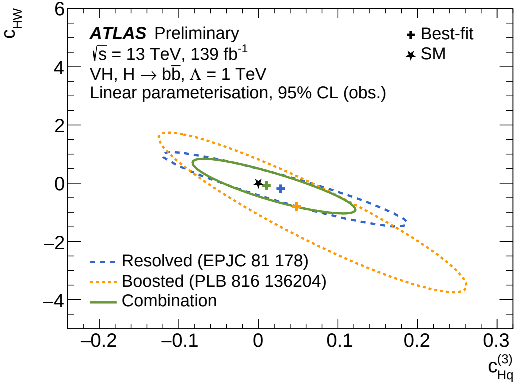

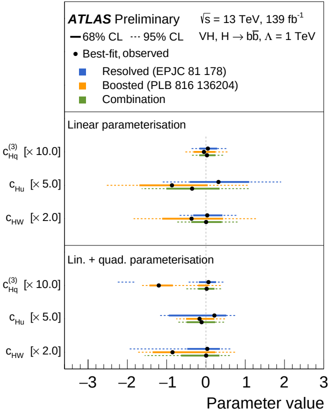

- Constraints on Wilson coefficients sensitive to modifiying $VH, H \to b\bar{b}$ production are placed at 95% CL (either 1 or 2 POI fits)

Combination strengthens limits w.r.t. individual analyses (particularly for parameters with strong energy dependence) and also resolves some ambiguities!

Exploit the high $H \to b\bar{b}$ decay rate to probe inclusive Higgs production at $p_T^H > 450$ GeV by targeting a boosted Higgs recoiling against a jet

- Select events with two large-R ($R = 1.0$) jets, one containing two b-tagged track sub-jets
- Large background from multi-jet production, modelled with parametric function, validated in 0 b-tag region (VRS/VRL, below)
- Smaller contributions from W/Z + jets and $t\bar{t}$, shapes modelled from simulation, $t\bar{t}$ normalisation constrained by CR

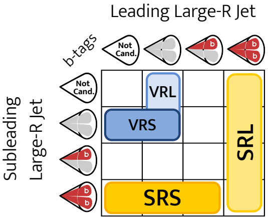

← Events categorised according to p_T of $H \to b\bar{b}$ candidate jet w.r.t. other jet

$H \to b\bar{b}$ jet mass used as S/B discriminant →

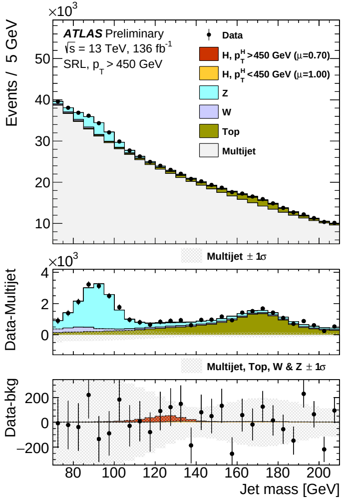

Measurement of high p_T $Z(b\bar{b})$ + jets production used to validate analysis methods

Boosted $H \to b\bar{b}$ (all-hadronic) (ATLAS-CONF-2021-010)

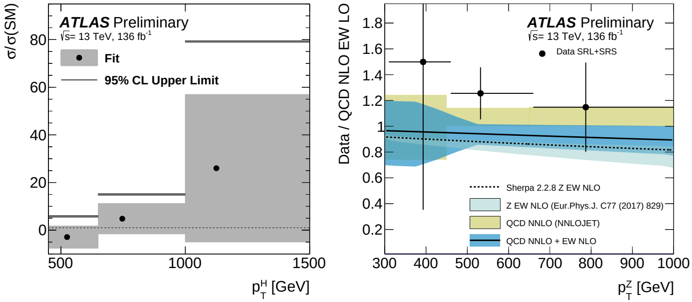

Signal strength measurements, performed differentially in p_T^H, for $H \to b\bar{b}$ (left) and $Z \to b\bar{b}$ (right)

p_T^H	μ_H	σ_H [fb]	
		Best fit	95% CL upper limit
> 450 GeV	0.7 ± 3.3	13 ± 52 (stat.) ± 32 (syst.) ± 3 (theory)	144
> 1 TeV	26 ± 31	3.4 ± 3.9 (stat.) ± 1.0 (syst.) ± 0.8 (theory)	10.3

Fiducial cross-section measurements performed in region matching experimental acceptance ($|\eta_H| < 2.0$, $p_T^H > 450$ GeV)

- $Z \to b\bar{b}$ validation measurements consistent with SM expectations, $H \to b\bar{b}$ sensitivity limited by statistical uncertainties

Sensitivity to high p_T^H Higgs production still quite far from SM prediction, but very relevant to exclude potential deviations in extreme regions of phase space

Search for $H \to b\bar{b}$ decays in VBF($+\gamma$) events with 126 - 132 fb^{-1} of 13 TeV data

All-hadronic Channel

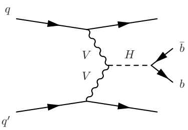

- Select events with two central *b*-tagged and two VBF-like jets
- Adversarial Neural Network (ANN) trained on kinematic variables used to define VBF rich categories and aid background modelling

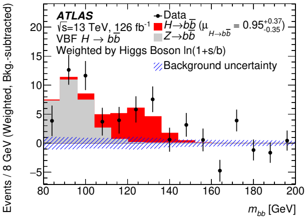

Photon Channel

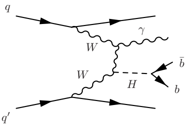

- Similar to all-hadronic channel with additional requirement of a reconstructed isolated photon
- Photon effective in reducing dominant gluon-rich *bbjj* background, enriching VBF purity

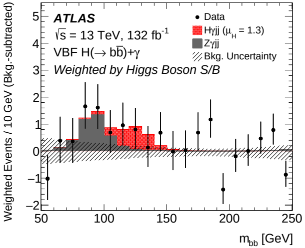

Background subtracted S/B weighted $m_{b\bar{b}}$ distributions shown for both channels ↑

The signal strength measurements for both analyses are statistically combined ↓

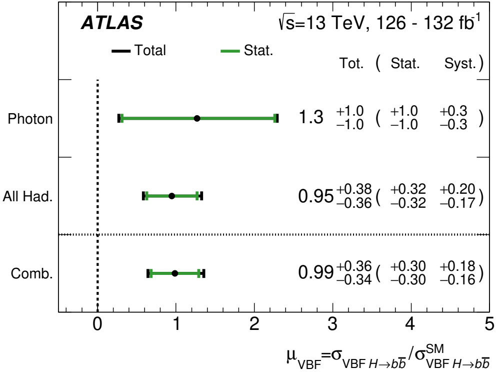

- Combined sensitivity driven by all-hadronic channel, both analyses limited by statistical uncertainties (particularly photon channel)
- In both cases, leading systematic uncertainties associated with modelling of non-resonant background (though methods differ)

$H \to b\bar{b}$ decay established at 3σ (expected and observed) in VBF channels alone!

The $H \to c\bar{c}$ decay offers a unique opportunity to directly probe the poorly constrained coupling of the Higgs boson to second generation quarks

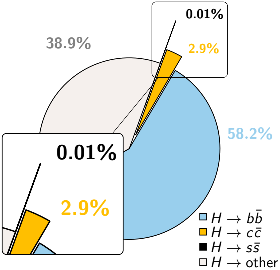

↑ 125 GeV SM Higgs boson branching fractions

- $H \to c\bar{c}$ now one of the largest contributions to Γ_H (by SM expectation) yet to be established experimentally!

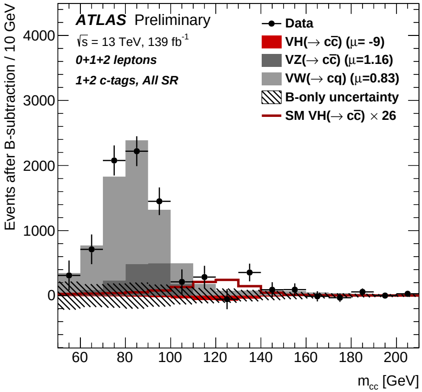

↑ Background subtracted di-jet invariant mass distributions for events with 1 or 2 c-tagged jets

Recently released ATLAS analysis, based on full Run 2 dataset ($139\,\text{fb}^{-1}$), exploits $(W/Z)H$ production and novel c-tagging to mitigate large multi-jet backgrounds

↓ 95% CL upper limits on the $VH, H \to c\bar{c}$ signal strength, from the three individual channels and combination

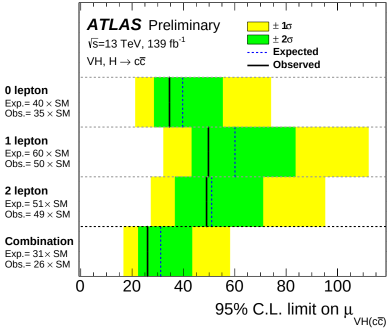

↓ Constraint on c-quark coupling modifier κ_c in a simple scenario where all other Higgs couplings are SM-like

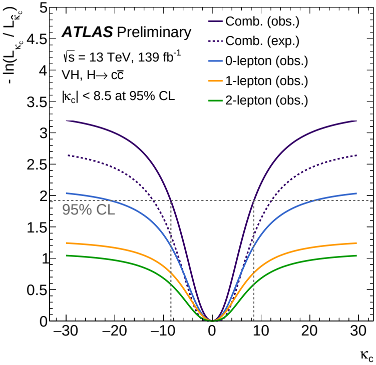

- Systematic uncertainties (primarily background modelling) limit sensitivity

$$\mu = \kappa_c^2 / \left(1 + \mathcal{B}(H \to c\bar{c}) \cdot (\kappa_c^2 - 1)\right)$$

Analysis now sensitive to $\mathcal{B}(H \to c\bar{c}) < 100\%$ allowing important direct coupling interpretation, constraint of $|\kappa_c| < 8.5$ at 95% CL observed

Complementary to indirect constraints from differential measurements of p_T^H with $H \to \gamma\gamma$ $(-19 < \kappa_c < 24)$ and $H \to 4\ell$ $(-12 < \kappa_c < 11)$

The $H \to \tau^+\tau^-$ decay represents the most sensitive probe of the Higgs boson's coupling to leptons, second most copious fermionic decay at $m_H = 125$ GeV!

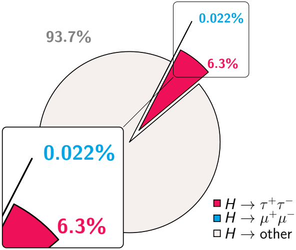

↑ **125 GeV SM Higgs boson branching fractions**

- ✓ High rate decay mode offers great opportunity to study the Yukawa mechanism in detail
- ✗ Complicated by experimental challenges associated with τ lepton decay reconstruction

Analysis Strategy

- Three decay channels considered: $\tau_{\text{had}}\tau_{\text{had}}$, $\tau_{\text{had}}\tau_{e,\mu}$ and $\tau_e\tau_\mu$
- Mitigate large $Z \to \tau^+\tau^-$ background with MVA production mode taggers
- Validate $Z \to \tau^+\tau^-$ modelling with MC using kinematic "embedding" technique
- Use "Missing Mass Calculator" (MMC) algorithm to improve $\tau^+\tau^-$ mass resolution, accounting neutrino energy losses

Recently released ATLAS analysis, based on full Run 2 dataset (139 fb^{-1}), uses novel production mode tagging methods to mitigate large $Z \to \tau^+\tau^-$ background

Design event categorisation strategy to optimise sensitivity and achieve good alignment with fiducial regions defined in STXS stage 1.2 scheme

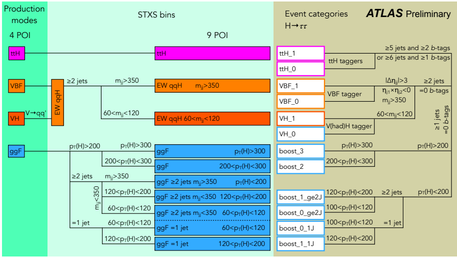

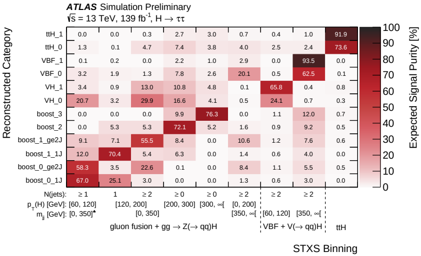

(left) Production mode fit POIs, STXS fit bins targeted and corresponding event categories (right) Relative contribution from signal in each reconstructed category to various STXS bins (i.e. rows sum to 100%)

- Four multivariate production mode taggers trained with kinematic, angular and τ property variables for: **VBF**, **V(had.)H**, **$t\bar{t}H$ (vs. $t\bar{t}$ or $Z \rightarrow \tau^+\tau^-$)**
- VBF, VH and $t\bar{t}H$ enriched regions defined and split into two categories ("_1" = enriched subset, "_0" = remainder)
- Six "boosted" categories defined by p_T^H and jet multiplicity target high p_T^H ggH production

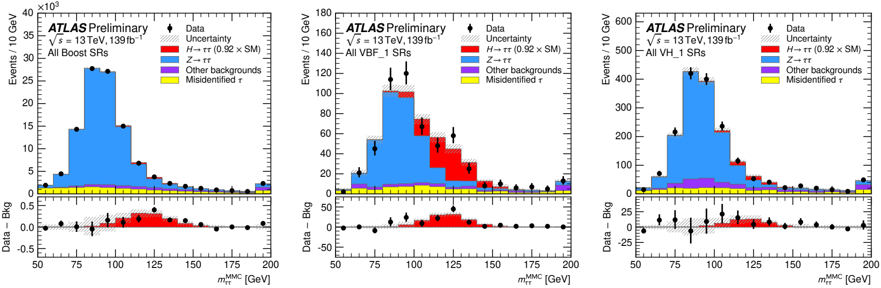

$m^{\mathrm{MMC}}_{\tau^+\tau^-}$ distributions for the sum of boosted (left) and individual purified VBF (centre) and VH (right) categories

- Dominant background is $Z \to \tau^+\tau^-$, modelled with MC and validated + normalised using $Z \to \ell\ell$ “embedding” control regions
- Background from misidentified τ estimated with fake factor ($\tau_{\mathrm{had.}}\tau_{e,\mu}$ and $\tau_{\mathrm{had.}}\tau_{\mathrm{had.}}$) and matrix ($\tau_e\tau_\mu$) methods
- Other backgrounds include $t\bar{t}$ (modelled with b-tagged jet CRs) and other minor EW processes (modelled with MC)

Binned likelihood fit performed to $m^{\mathrm{MMC}}_{\tau^+\tau^-}$ distributions of 32 signal and 36 control ($Z \to \ell\ell$ “embedding” and $t\bar{t}$) regions in 1 (inclusive), 4 (prod. mode) and 9 (STXS) POI configurations

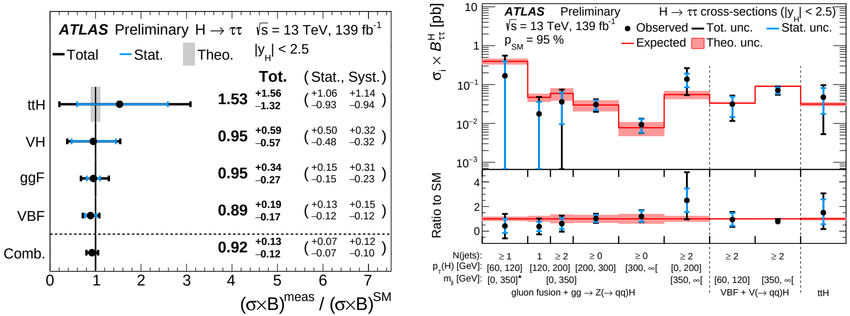

Inclusive and production mode signal strength measurements (left) and STXS fiducial cross-sections (right)

- Both STXS and production mode measurements very consistent with SM predictions
- Systematic uncertainties generally dominated by signal theory uncertainties

VBF and *ggH* production established using $H \to \tau^+\tau^-$ decays alone, with observed (expected) significances of 5.3 (6.2) σ and 3.9 (4.6) σ, respectively!

Most promising probe of Higgs coupling to second generation fermions, now approaching sensitivity to test SM prediction!

- Dominant backgound is $Z \to \mu^+\mu^-(+\text{jets})$, important to exploit multiple production modes
- In events with exactly two muons, classify with BDTs trained with production mode sensitive variables

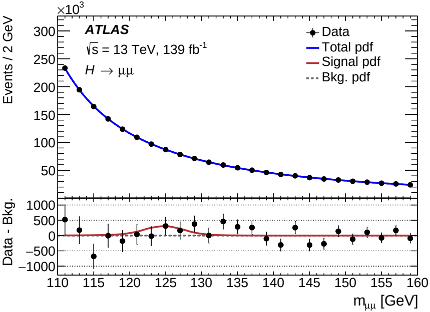

↑ **Di-muon invariant mass distribution for the sum of all categories, background modelled with empirical functions**

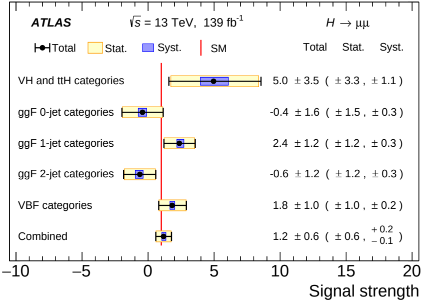

- Sensitivity driven by VBF targetted categories, still very much limited by statistical uncertainties
- Observed (expected) significance $2.0\,(1.7)\,\sigma$ (w.r.t B only)

Don't forget $H \to e^+e^-$!

$\mathcal{B} < 3.6 \times 10^{-4}$ (PLB 801 (2020) 135148)

ATLAS is using the 139 fb^{-1} 13 TeV Run 2 dataset to considerably advance our understanding of the Higgs boson's couplings to the fermions!

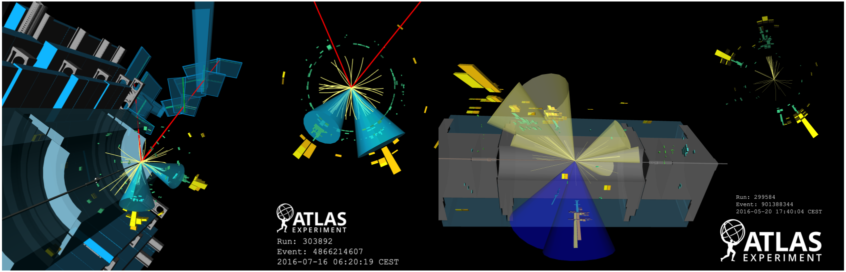

Candidate $Z(\mu^+\mu^-)H(c\bar{c})$ ↖ and fully-hadronic $t\bar{t}H(\tau^+\tau^-)$ ↗ events

Higgs boson couplings to third generation fermions are now very well established, no discrepencies observed w.r.t. SM predictions

- The $H \to b\bar{b}$ and $H \to \tau^+\tau^+$ decays are now being extensively used as tools to study Higgs boson production at the LHC in ever increasing detail

Could a surprise be lurking in the first two generation's couplings? Exciting progress being made towards probing couplings to second generation fermions

- Sensitivity to $H \to \mu^+\mu^-$ approaching level where SM prediction can be tested
- Latest search for $H \to c\bar{c}$ decays dramatically advances constraint on κ_c

Additional Slides

Strategy closely linked to ATLAS $VH, H \to b\bar{b}$ analyses and based on 3 channels:

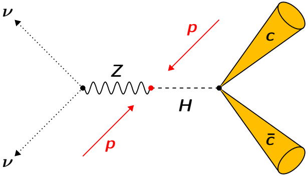

← 0 lepton channel

- Target the $Z(\nu\nu)H(c\bar{c})$ signature
- Large $E_{\mathrm{T}}^{\mathrm{miss}}$ (consistent with $Z \to \nu\nu$) and at least two jets (≥ 1 c-tag)

1 lepton channel →

- Target the $W(\ell\nu)H(c\bar{c})$ signature
- Exactly one lepton (e or μ) and $E_{\mathrm{T}}^{\mathrm{miss}}$ (consistent with $W \to \ell\nu$) and at least two jets (≥ 1 c-tag)

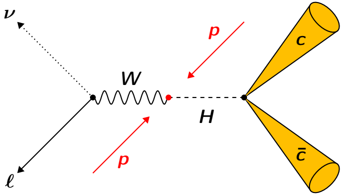

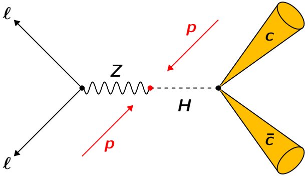

← 2 lepton channel

- Target the $Z(\ell\ell)H(c\bar{c})$ signature
- Exactly two leptons (e^+e^- or $\mu^+\mu^-$) (consistent with $Z \to \ell\ell$) and at least two jets (≥ 1 c-tag)

Perform cut-based analysis, use di-jet mass $m_{c\bar{c}}$ as primary S/B discriminant and exploit c-tagging to target the $H \to c\bar{c}$ signal and suppress backgrounds...

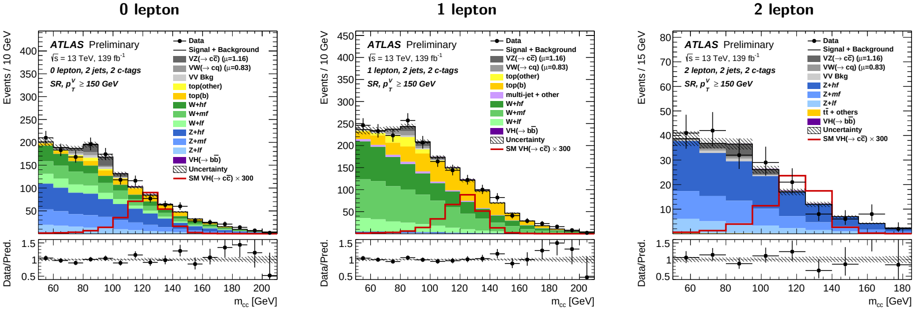

↑ **Di-jet invariant mass distributions for 2 c-tag categories, in each of the channels**

- Events categorised by p_{T}^{V}, jet multiplicity and c-tag multiplicity
- Background dominated by W/Z+jets and $t\bar{t}$ (in 0/1 lepton channels), with sub-leading contributions from VW and VZ production
- Dedicated control regions to constrain W/Z+jets (high ΔR_{jj} events) and $t\bar{t}$ (1 c-tag, with b-tagged third jet) background modelling in data

Binned likelihood fit performed to $m_{c\bar{c}}$ distributions of the 44 analysis regions with three signal strength POIs: $VH, H \rightarrow c\bar{c}$, $VZ, Z \rightarrow c\bar{c}$, $VW, W \rightarrow cq$

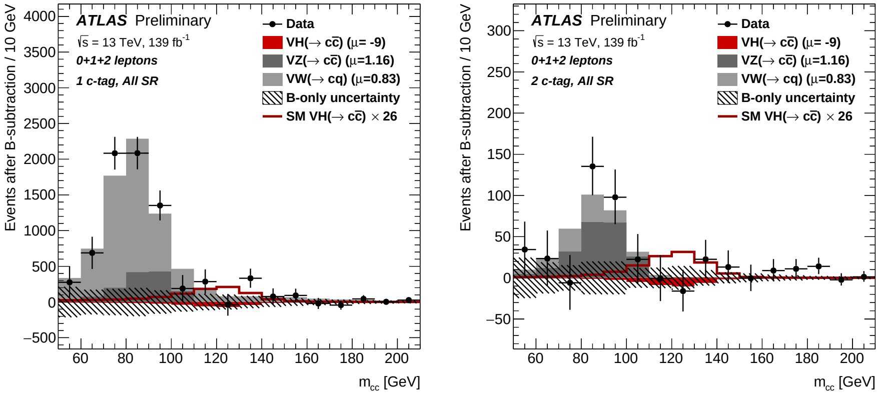

↑ **Background subtracted di-jet invariant mass distributions for events with 1 (left) or 2 (right) *c*-tagged jets**

- Methodology validated with inclusive $VZ(c\bar{c})$ and $VW(cq)$ production
- Signal strength parameters measured to be consistent with SM with observed (expected) significance of **2.6 (2.2)** σ and **3.8 (4.6)** σ, respectively

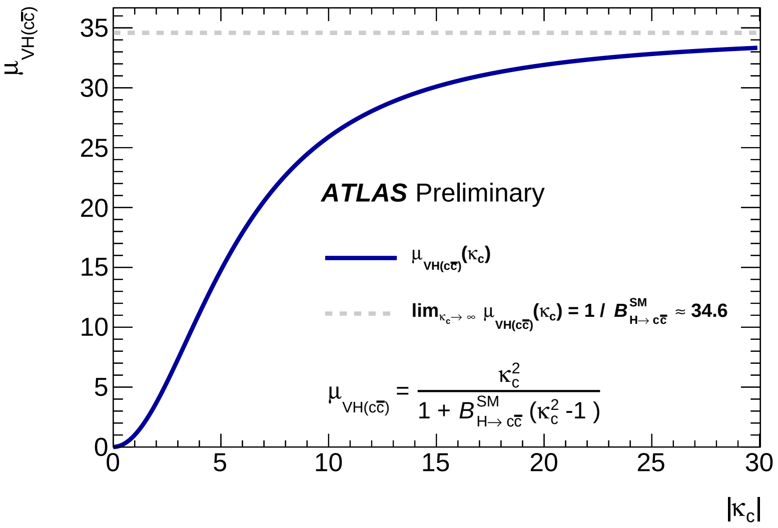

$\mu_{VH(c\bar{c})}$
0
5
10
15
20
25
30
35
0
5
10
15
20
25
30
$|\kappa_c|$
ATLAS Preliminary
$\mu_{VH(c\bar{c})}(\kappa_c)$
$\lim_{\kappa_c \to \infty} \mu_{VH(c\bar{c})}(\kappa_c) = 1 / B^{SM}_{H \to c\bar{c}} \approx 34.6$
$\mu_{VH(c\bar{c})} = \frac{\kappa_c^2}{1 + B^{SM}_{H \to c\bar{c}} (\kappa_c^2 - 1)}$

$VH, H \to c\bar{c}$ - Uncertainty Breakdown (ATLAS-CONF-2021-021)

Source of uncertainty		$\mu_{VH(c\bar{c})}$	$\mu_{VW(cq)}$	$\mu_{VZ(c\bar{c})}$
Total		15.3	0.24	0.48
Statistical		10.0	0.11	0.32
Systematics		11.5	0.21	0.36
Statistical uncertainties				
Data statistics only		7.8	0.05	0.23
Floating normalisations		5.1	0.09	0.22
Theoretical and modelling uncertainties				
$VH(\to c\bar{c})$		2.1	< 0.01	0.01
Z+jets		7.0	0.05	0.17
Top-quark		3.9	0.13	0.09
W+jets		3.0	0.05	0.11
Diboson		1.0	0.09	0.12
$VH(\to b\bar{b})$		0.8	< 0.01	0.01
Multi-Jet		1.0	0.03	0.02
Simulation statistics		4.2	0.09	0.13
Experimental uncertainties				
Jets		2.8	0.06	0.13
Leptons		0.5	0.01	0.01
$E_{\mathrm{T}}^{\mathrm{miss}}$		0.2	0.01	0.01
Pile-up and luminosity		0.3	0.01	0.01
Flavour tagging	c-jets	1.6	0.05	0.16
	b-jets	1.1	0.01	0.03
	light-jets	0.4	0.01	0.06
	τ-jets	0.3	0.01	0.04
Truth-flavour tagging	ΔR correction	3.3	0.03	0.10
	Residual non-closure	1.7	0.03	0.10

$VH(\to b\bar{b})$	
$WH(\to b\bar{b})$ normalisation	27%
$ZH(\to b\bar{b})$ normalisation	25%
Diboson	
$WW/ZZ/WZ$ acceptance	10/5/12%
p_{T}^{V} acceptance	4%
N_{jet} acceptance	7 – 11%
Z+jets	
Z+hf normalisation	Floating
Z+mf normalisation	Floating
Z+lf normalisation	Floating
$Z+bb$ to $Z+cc$ ratio	20%
$Z+bl$ to $Z+cl$ ratio	18%
$Z+bc$ to $Z+cl$ ratio	6%
p_{T}^{V} acceptance	1 – 8%
N_{jet} acceptance	10 – 37%
High ΔR CR to SR	12 – 37%
0- to 2-lepton ratio	4 – 5%
W+jets	
W+hf normalisation	Floating
W+mf normalisation	Floating
W+lf normalisation	Floating
$W+bb$ to $W+cc$ ratio	4 – 10 %
$W+bl$ to $W+cl$ ratio	31 – 32 %
$W+bc$ to $W+cl$ ratio	31 – 33 %
$W\to\tau\nu(+c)$ to $W+cl$ ratio	11%
$W\to\tau\nu(+b)$ to $W+cl$ ratio	27%
$W\to\tau\nu(+l)$ to $W+l$ ratio	8%
N_{jet} acceptance	8 – 14%
High ΔR CR to SR	15 – 29%
$W\to\tau\nu$ SR to high ΔR CR ratio	5 – 18%
0- to 1-lepton ratio	1 – 6 %
Top quark (0- and 1-lepton)	
top(b) normalisation	Floating
top(other) normalisation	Floating
N_{jet} acceptance	7 – 9%
0- to 1-lepton ratio	4%
SR/top CR acceptance ($t\bar{t}$)	9%
SR/top CR acceptance (Wt)	16%
Wt / $t\bar{t}$ ratio	10%
Top quark (2-lepton)	
Normalisation	Floating
Multi-jet (1-lepton)	
Normalisation	20 – 100%

Latest measurements with full Run 2 dataset deliver most precise measurements of VH production and firmly establish $H \to b\bar{b}$ decay (6.7σ)!

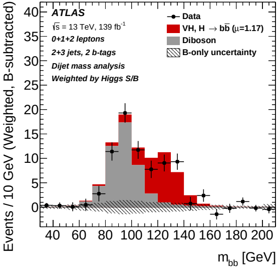

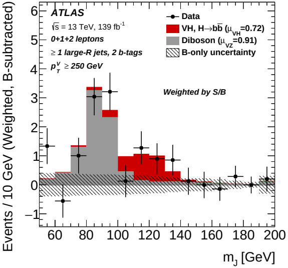

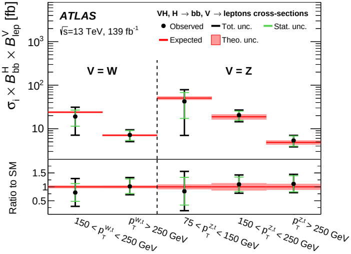

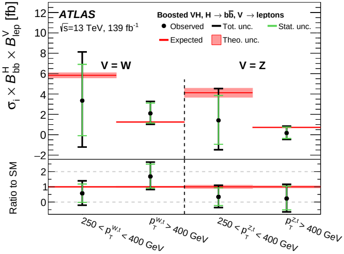

Resolved (left) and boosted (right) $H \to b\bar{b}$ mass distributions and STXS measurements of WH and ZH production

$H \to b\bar{b}$ with VBF (inclusive), uncertainties (EPJC 81 (2021) 537)

Uncertainty	$\sigma(\mu_{H\to b\bar{b}})$
Statistics	± 0.31
NR Background Bias	± 0.15
Embedded Z	± 0.05
Experimental	$+0.10/-0.05$
Trigger	$+0.07/-0.03$
Jet	$+0.06/-0.04$
Flavor Tagging	$+0.02/-0.01$
Other	$+0.02/-0.01$
Signal Theory	$+0.06/-0.03$

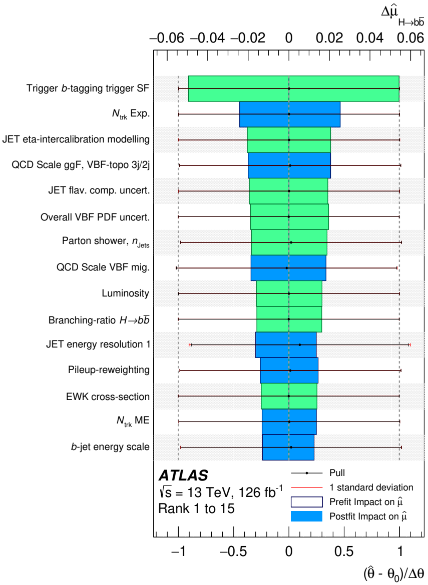

$H \to b\bar{b}$ with VBF (inclusive), fit (EPJC 81 (2021) 537)

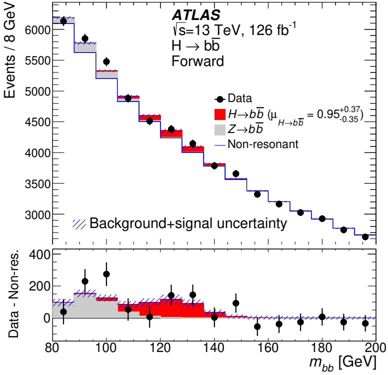

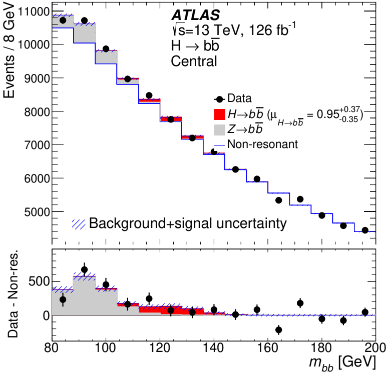

$H \to b\bar{b}$ with VBF (inclusive), ANN (EPJC 81 (2021) 537)

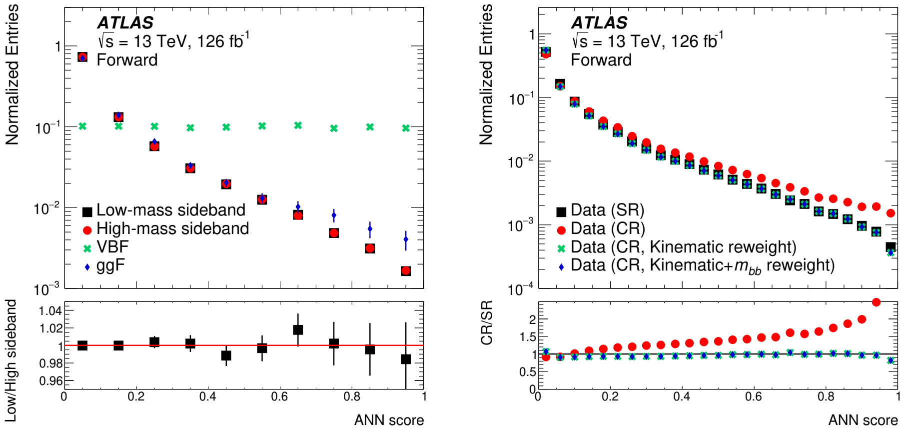

Source of absolute uncertainty	$\sigma(\mu_H)$ down	$\sigma(\mu_H)$ up
Statistical		
Data statistical	-0.78	$+0.80$
Bkg. fit shapes	-0.19	$+0.22$
Bkg. fit normalizations	-0.51	$+0.52$
Z boson normalizations	-0.15	$+0.14$
Systematic		
Spurious signal	-0.24	$+0.21$
Theoretical	-0.01	$+0.08$
Photon	-0.01	$+0.03$
Jet	-0.06	$+0.20$
b-tagging	-0.02	$+0.11$
Auxiliary	-0.01	$+0.04$
Total	-0.99	$+1.04$
Total statistical	-0.96	$+0.99$
Total systematic	-0.25	$+0.32$

$H \to b\bar{b}$ with VBF (photon), BDT (JHEP 03 (2021) 268)

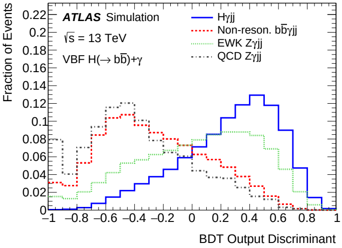

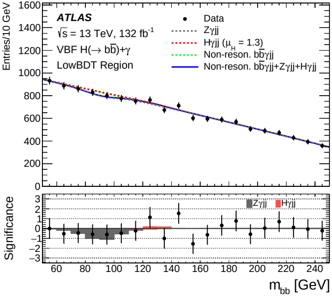

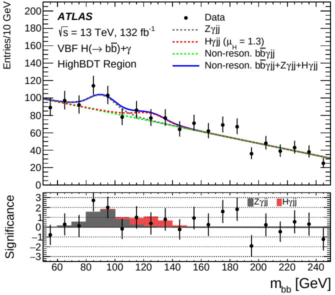

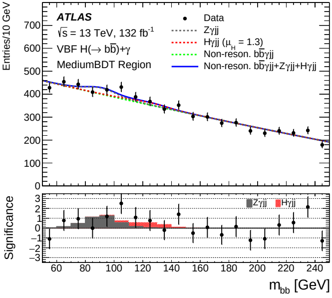

$H \to \tau^+\tau^-$, selection (ATLAS-CONF-2021-044)

	$\tau_e\tau_\mu$	$\tau_{\text{lep}}\tau_{\text{had}}$		$\tau_{\text{had}}\tau_{\text{had}}$
		$\tau_e\tau_{\text{had}}$	$\tau_\mu\tau_{\text{had}}$	
N(e)	1	1	0	0
N(μ)	1	0	1	0
N($\tau_{\text{had-vis}}$)	0	1	1	2
e p_{T} cut [GeV]	27, 15, 18	27		
μ p_{T} cut [GeV]	10, 27.3, 14.7		27.3	
$\tau_{\text{had-vis}}$ p_{T} cut [GeV]		30		40, 30
Identification	e/μ: Medium	$e/\mu/\tau_{\text{had-vis}}$: Medium		$\tau_{\text{had-vis}}$: Medium
Isolation	e: Loose μ: Tight	e: Loose	μ: Tight	
Charge	Opposite charge	Opposite charge		Opposite charge
Kinematics	$m_{\tau\tau}^{\text{coll}} > m_Z - 25\,\text{GeV}$ $30\,\text{GeV} < m_{e\mu} < 100\,\text{GeV}$	$m_{\text{T}} < 70\,\text{GeV}$		
b-veto	# of b-jets = 0	# of b-jets = 0		# of b-jets = 0 (≥ 1 or 2 in ttH categories)
$E_{\text{T}}^{\text{miss}}$	$E_{\text{T}}^{\text{miss}} > 20\,\text{GeV}$	$E_{\text{T}}^{\text{miss}} > 20\,\text{GeV}$		$E_{\text{T}}^{\text{miss}} > 20\,\text{GeV}$
Leading jet	$p_{\text{T}} > 40\,\text{GeV}$	$p_{\text{T}} > 40\,\text{GeV}$		$p_{\text{T}} > 70\,\text{GeV}$, $\lvert\eta\rvert < 3.2$
Angular	$\Delta R_{e\mu} < 2.0$ $\lvert\Delta\eta_{e\mu}\rvert < 1.5$	$\Delta R_{\ell\tau_{\text{had-vis}}} < 2.5$ $\lvert\Delta\eta_{\ell\tau_{\text{had-vis}}}\rvert < 1.5$		$0.6 < \Delta R_{\tau_{\text{had-vis}}\tau_{\text{had-vis}}} < 2.5$ $\lvert\Delta\eta_{\tau_{\text{had-vis}}\tau_{\text{had-vis}}}\rvert < 1.5$
Coll. app. x_1/x_2	$0.1 < x_1 < 1.0$ $0.1 < x_2 < 1.0$	$0.1 < x_1 < 1.4$ $0.1 < x_2 < 1.2$		$0.1 < x_1 < 1.4$ $0.1 < x_2 < 1.4$

	Variable	VBF	V(had)H	ttH vs $t\bar{t}$	ttH vs $Z \to \tau\tau$
Jet properties	Invariant mass of 2 leading jets	•	•		
	$p_T(jj)$	•	•		
	Product of η of 2 leading jets	•			
	Sub-leading jet p_T	•			
	Leading jet η				•
	Sub-leading jet η				•
	Scalar sum of all jets p_T			•	•
	Scalar sum of all b-tagged jets p_T				•
	Best W-candidate dijet invariant mass			•	•
	Best t-quark-candidate three-jet invariant mass			•	•
Angular distances	$\Delta\phi$(jet 0, jet 1)	•			
	$\|\Delta\eta$(jet 0, jet 1)$\|$	•	•		
	ΔR(jet 0, jet 1)		•		
	$\Delta R(\tau\tau, jj)$		•		
	$\Delta R(\tau, \tau)$		•	•	
	Smallest ΔR (any 2 jets)			•	
	$\|\Delta\eta(\tau, \tau)\|$			•	•
τ prop.	$p_T(\tau\tau)$			•	
	Sub-leading τ p_T				•
	Sub-leading τ η				•
H cand.	$p_T(Hjj)$	•	•		
	$p_T(H)/p_T(jj)$		•		
$\vec{E}_T^{miss}$	Missing transverse energy E_T^{miss}		•	•	•
	Smallest $\Delta\phi$ $(\tau, \vec{E}_T^{miss})$				•

$H \to \tau^+\tau^-$, uncertainties (ATLAS-CONF-2021-044)

Source of uncertainty	Impact on $\Delta\sigma\,/\,\sigma(pp \to H \to \tau\tau)$ [%] Observed	Expected
Theoretical uncertainty in signal	8.1	8.6
Jet and $\vec{E}_{\mathrm{T}}^{\mathrm{miss}}$	4.2	4.1
Background sample size	3.7	3.4
Hadronic τ decays	2.0	2.1
Misidentified τ	1.9	1.8
Luminosity	1.7	1.8
Theoretical uncertainty in Top processes	1.4	1.2
Theoretical uncertainty in Z+jets processes	1.1	1.1
Flavor tagging	0.5	0.5
Electrons and muons	0.4	0.3
Total systematic uncertainty	11.1	11.0
Data sample size	6.6	6.3
Total	12.8	12.5

Fiducial Measurements

Process	$p_T^H > 450$ GeV	$p_T^H > 1$ TeV
All	0.25	0.18
ggF	0.26	0.22
VH	0.27	0.19
VBF	0.22	0.15
ttH	0.20	0.16

↑ Acceptance × efficiency

Uncertainty Contribution	$p_T^H > 450$ GeV	$p_T^H > 1$ TeV
Total	3.3	31
Statistical	2.8	30
Jet Systematics	1.2	7
Modeling and Theory Systs.	1.0	1
Flavor Tagging Systs.	0.5	3
Total Systematics	1.7	8

↑ Uncertainty Breakdown

Differential Measurements

Process	$300 < p_T^H < 450$ GeV	$450 < p_T^H < 650$ GeV	$p_T^H > 650$ GeV
All	1.4×10^{-2}	0.25	0.33
ggF	0.7×10^{-2}	0.26	0.37
VH	1.8×10^{-2}	0.28	0.31
VBF	0.2×10^{-2}	0.14	0.18
$t\bar{t}H$	4.9×10^{-2}	0.20	0.25

↑ Acceptance × efficiency

Uncertainty Contribution	$300 < p_T^H < 450$ GeV	$450 < p_T^H < 650$ GeV	$p_T^H > 650$ GeV
Total	17	4.7	6.4
Statistical	16	4.0	5.9
Jet Systematics	5.4	2.6	2.3
Modeling and Theory Systs.	3.8	< 0.1	0.1
Flavor Tagging Systs.	< 0.1	< 0.1	< 0.1
Total Systematics	6	2.7	2.5

↑ Uncertainty Breakdown

VH, $H \to b\bar{b}$ Combination (ATLAS-CONF-2021-051)

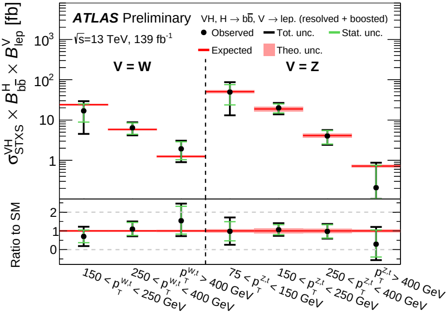

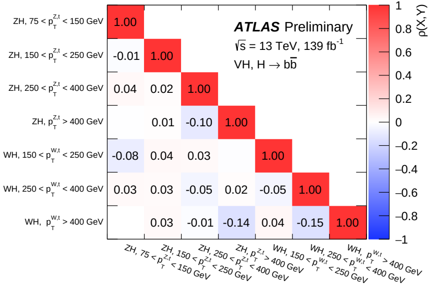

$VH, H \to b\bar{b}$ Combination (ATLAS-CONF-2021-051)

ATLAS Simulation Preliminary $\sqrt{s}$ = 13 TeV

Signal fraction [%]

	WH, $p_T^{W,t}$ < 150 GeV	WH, 150 < $p_T^{W,t}$ < 250 GeV	WH, 250 < $p_T^{W,t}$ < 400 GeV	WH, $p_T^{W,t}$ > 400 GeV	ZH, $p_T^{Z,t}$ < 75 GeV	ZH, 75 < $p_T^{Z,t}$ < 150 GeV	ZH, 150 < $p_T^{Z,t}$ < 250 GeV	ZH, 250 < $p_T^{Z,t}$ < 400 GeV	ZH, $p_T^{Z,t}$ > 400 GeV
2 lep, p_T^V > 400 GeV, boosted SR								4.9	95.1
2 lep, ≥ 3 jets, 250 < p_T^V < 400 GeV							3.8	95.0	1.1
2 lep, 2 jets, 250 < p_T^V < 400 GeV							3.8	95.1	1.1
2 lep, ≥ 3 jets, 150 < p_T^V < 250 GeV						2.0	96.3	1.6	
2 lep, 2 jets, 150 < p_T^V < 250 GeV						2.4	96.2	1.4	
2 lep, ≥ 3 jets, 75 < p_T^V < 150 GeV					1.0	96.7	2.2		
2 lep, 2 jets, 75 < p_T^V < 150 GeV					1.1	97.2	1.7		
0 lep, p_T^V > 400 GeV, boosted LP SR			0.7	20.3				7.4	71.5
0 lep, p_T^V > 400 GeV, boosted HP SR			0.7	16.9				7.2	75.3
0 lep, 3 jets, 250 < p_T^V < 400 GeV		1.3	12.9	3.3			10.3	67.8	4.3
0 lep, 2 jets, 250 < p_T^V < 400 GeV		0.9	13.7	4.1			7.6	68.6	5.1
0 lep, 3 jets, 150 < p_T^V < 250 GeV	1.9	15.2	4.7	0.2		8.5	62.7	6.6	0.1
0 lep, 2 jets, 150 < p_T^V < 250 GeV	1.4	15.1	5.0	0.3		7.4	63.4	7.3	0.1
1 lep, p_T^V > 400 GeV, boosted LP SR			8.5	90.1				0.1	1.4
1 lep, p_T^V > 400 GeV, boosted HP SR			8.2	90.9					0.9
1 lep, 3 jets, 250 < p_T^V < 400 GeV	0.1	10.9	80.7	6.3			0.2	1.4	0.4
1 lep, 2 jets, 250 < p_T^V < 400 GeV		8.4	83.2	7.1			0.1	1.0	0.2
1 lep, 3 jets, 150 < p_T^V < 250 GeV	11.1	75.9	9.2	0.1		0.5	2.4	0.7	0.1
1 lep, 2 jets, 150 < p_T^V < 250 GeV	8.4	79.0	10.1	0.1		0.3	1.6	0.4	

ATLAS Simulation Preliminary $\sqrt{s}$ = 13 TeV, 139 fb^{-1}

Signal events

	WH, $p_T^{W,t}$ < 150 GeV	WH, 150 < $p_T^{W,t}$ < 250 GeV	WH, 250 < $p_T^{W,t}$ < 400 GeV	WH, $p_T^{W,t}$ > 400 GeV	ZH, $p_T^{Z,t}$ < 75 GeV	ZH, 75 < $p_T^{Z,t}$ < 150 GeV	ZH, 150 < $p_T^{Z,t}$ < 250 GeV	ZH, 250 < $p_T^{Z,t}$ < 400 GeV	ZH, $p_T^{Z,t}$ > 400 GeV
2 lep, p_T^V > 400 GeV, boosted SR								0.2	3.6
2 lep, ≥ 3 jets, 250 < p_T^V < 400 GeV							0.8	20.7	0.2
2 lep, 2 jets, 250 < p_T^V < 400 GeV							0.3	8.4	0.1
2 lep, ≥ 3 jets, 150 < p_T^V < 250 GeV						1.6	74.0	1.2	
2 lep, 2 jets, 150 < p_T^V < 250 GeV						0.8	33.8	0.5	
2 lep, ≥ 3 jets, 75 < p_T^V < 150 GeV					1.2	124.7	2.9		
2 lep, 2 jets, 75 < p_T^V < 150 GeV					0.9	78.4	1.4		
0 lep, p_T^V > 400 GeV, boosted LP SR			0.1	1.5				0.6	5.4
0 lep, p_T^V > 400 GeV, boosted HP SR			0.1	1.3				0.6	6.0
0 lep, 3 jets, 250 < p_T^V < 400 GeV		0.4	4.4	1.1			3.6	23.3	1.5
0 lep, 2 jets, 250 < p_T^V < 400 GeV		0.3	4.8	1.4			2.7	24.2	1.8
0 lep, 3 jets, 150 < p_T^V < 250 GeV	2.8	22.6	7.0	0.3		12.5	93.0	9.8	0.1
0 lep, 2 jets, 150 < p_T^V < 250 GeV	2.1	22.6	7.5	0.5		11.0	95.0	10.9	0.1
1 lep, p_T^V > 400 GeV, boosted LP SR			0.8	8.8					0.1
1 lep, p_T^V > 400 GeV, boosted HP SR			0.9	9.8					0.1
1 lep, 3 jets, 250 < p_T^V < 400 GeV		4.8	35.4	2.8			0.1	0.6	0.2
1 lep, 2 jets, 250 < p_T^V < 400 GeV		3.8	37.2	3.2				0.4	0.1
1 lep, 3 jets, 150 < p_T^V < 250 GeV	16.2	110.5	13.4	0.1		0.7	3.5	1.0	0.1
1 lep, 2 jets, 150 < p_T^V < 250 GeV	12.7	118.6	15.1	0.2		0.4	2.4	0.6	

$VH, H \to b\bar{b}$ Combination (ATLAS-CONF-2021-051)

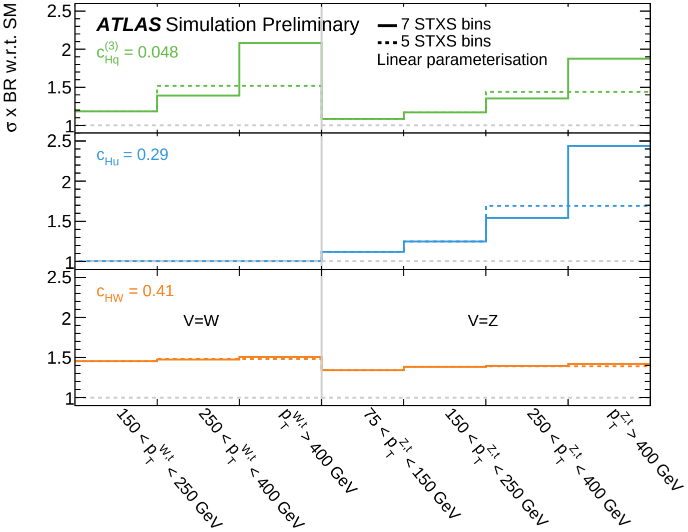

$VH, H \to b\bar{b}$ Combination (ATLAS-CONF-2021-051)

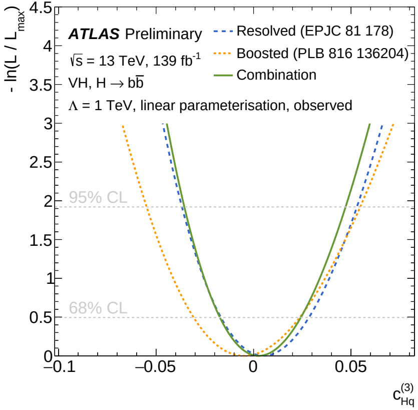

$VH, H \to b\bar{b}$ Combination (ATLAS-CONF-2021-051)